Simulation of Stomach Specimens Generation Based on Deformation of Preoperative CT Images

TrungDung Truong, Takayuki Kitasaka, Kensaku Mori, and Yasuhito Suenaga

Graduate School of Information Science, Nagoya University,
Furo-cho, Chikusa-ku, Nagoya 464-8603, Japan
ttdung@suenaga.m.is.nagoya-u.ac.jp,
{kitasaka, kensaku, suenaga}@is.nagoya-u.ac.jp

Abstract. This paper presents a novel method for generating virtually-unfolded views of the stomach by cutting and deforming CT images. Unfolded views are very useful for the diagnosis and treatment planning of stomach cancer, since they provide various information of the lumen which can only be obtained from a resected specimen. However, conventional methods cannot correctly reproduce luminal surfaces because elasticity for the shape model of the stomach is quite coarse defined. In this paper, we use Voigt elements for elasticity modeling, forces calculated from surface normals for directing the stomach to a flat shape, and the Newmark-β method for image deformation. We simulated deformation of a phantom dataset and compared the stability as well as computation time with the Euler method. Unfolded views from fifteen CT image datasets, corresponding virtual gastroscopic images, and resected specimens were used for comparison with conventional methods. Experimental results showed that our method can generate views faster in which concave regions of the stomach are better flattened and 99% of the luminal surface can be reproduced. Unfolded views from twelve datasets were presented for surgical planning. They were considered to have well reproduced lesions as well as fold patterns observed in virtual gastroscopic images and resected specimens.

1 Introduction

Virtual gastroscopy is now becoming an extremely gentle method for the early detection of stomach cancer as well as the follow-up examinations without putting too much strain on the patient [1]. However, because the stomach usually has a large cavity, virtual gastroscopy requires frequent change of viewpoints and view directions to confirm whether all regions of interest have been observed. It would be easier for observation if we could draw the entire lumen onto a planar surface. Mori et al. have shown that unfolded stomach views can be generated by cutting and deforming CT image data [2]. A number of approaches for unfolding the colon [3] or blood vessels [4] have also been developed.

Image deformation based unfolding requires both deforming the stomach to a flat shape and correct reconstruction of image data based on shape. Deformation

M. Harders and G. Székely (Eds.): ISBMS 2006, LNCS 4072, pp. 178–187, 2006.

of biological tissues can be accurately simulated by the finite element method (FEM)[5]. However, since the FEM requires remeshing for topological changes and is computationally expensive, it is not suitable for unfolding which definitely accompanies cutting and large deformation. Mori et al. [2] used a node-spring model to represent a stomach model whose deformation is computed as the movement of individual nodes under external forces. However, because elasticity for the model is quite coarse defined, their method cannot reproduce the luminal surface correctly. In this paper, we present a novel method that uses mass points and Voigt elements for elastic modeling, surface normals driven forces for directing the stomach to a flat shape, and the Newmark-β method [7] for image deformation. We believe our method could generate views in which the stomach wall is unfolded better and its luminal surface is reproduced more accurately. We will also show that our method can simulate stable deformation of soft tissues without modifying (or adding constraints to) mass point motion such as most conventional approaches using the Euler method usually do.

In Section 2, detailed procedures of our method are presented. Experimental results of simulating deformation of a phantom dataset and unfolding the stomach from preoperative CT images are shown in Section 3, where discussion is also stated.

2 Method

Unfolded views can be generated by deforming the stomach wall region in a CT image dataset and then visualizing the deformed dataset by volume rendering. Our method consists of six steps : (1) segmentation of the stomach wall, (2) generating a stomach model, (3) cutting and stretching the model, (4) flattening the model to a flat shape, (5) reconstructing image data, and (6) visualizing the reconstructed data. Steps (1), (5) and (6) are performed by exactly applying the conventional method [2], thus we do not describe them in this paper.

2.1 Our Stomach Model

Our stomach model consists of a set of hexahedra wrapping the stomach wall region in a CT image dataset. Each hexahedron is located so that its center coincides with the location of a voxel. The lengths of hexahedron edges in the x, y, and z directions are d, d, and d' ($d' = d \times \mathit{slice\ interval/pixel\ pitch}$), respectively, where d is an interger. Mass points are allocated at vertices of the hexahedra. Voigt elements are allocated along each edge and across the diagonals of each face (Fig. 1). Two hexahedra allocated at two adjacent voxels share one face including four mass points and four Voigt elements.

The equation of motion for a mass point i at time t can be represented by

$$m_i \mathbf{a}_i(t) = \mathbf{Fe}_i(t) + \sum_{j \in S_i} \mathbf{Fs}_{ij}(t), \tag{1}$$

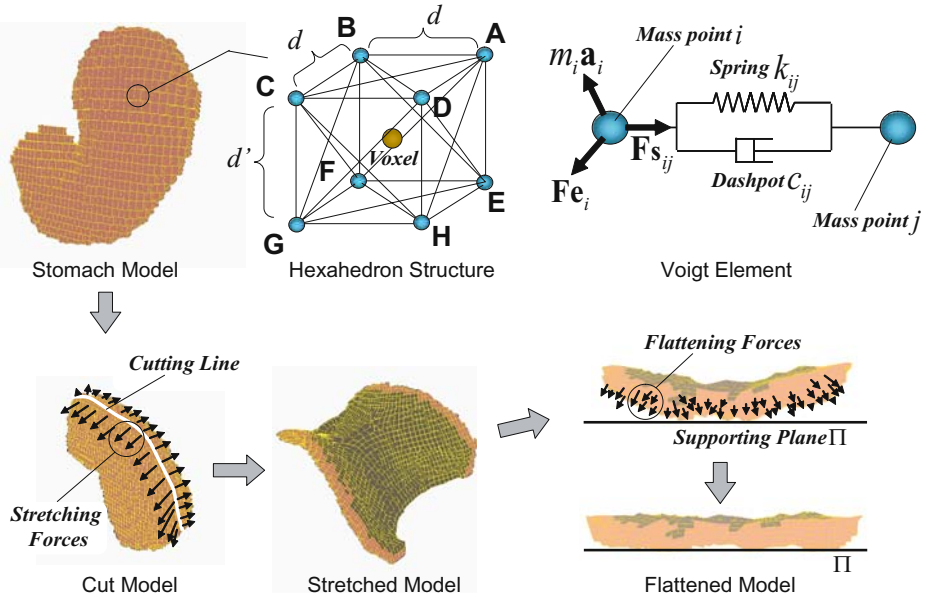

Fig. 1. Cutting, stretching and flattening the stomach model

where m_i and $\mathbf{a}_i(t)$ denote the mass and the acceleration of the mass point. $\mathbf{Fe}_i(t)$ is the external force working on the mass point. S_i denotes a set of mass points connected to i by Voigt elements. $\mathbf{Fs}_{ij}(t)$, the internal force by the Voigt element connecting mass points i and j, is formulated as

$$\mathbf{Fs}_{ij}(t) = k_{ij}\left(1 - \frac{\|\mathbf{r}_{ij}(0)\|}{\|\mathbf{r}_{ij}(t)\|}\right)\mathbf{r}_{ij}(t) + c_{ij}\mathbf{v}_{ij}(t), \tag{2}$$

where $\mathbf{r}_{ij}(t)$ and $\mathbf{v}_{ij}(t)$ represent the position and the velocity of j relative to i. k_{ij} and c_{ij} are the spring and damping constants.

Motion of the stomach is achieved by discretizing Eq. 1 using the Newmark-β method and then computing the acceleration, the velocity, and the position of mass points. By using a time step Δt, at time $t^{(n+1)} = (n+1)\Delta t$ $(n = 0, 1, 2, ...)$, acceleration $\mathbf{a}_i^{(n+1)}$, velocity $\mathbf{v}_i^{(n+1)}$, and position $\mathbf{r}_i^{(n+1)}$ of mass point i can be computed as

$$\mathbf{a}_i^{(n+1)} = \frac{\sum_{j\in S_i}\left[k_{ij}\left(1 - \frac{\|\mathbf{r'}_{ij}^{(0)}\|}{\|\mathbf{r'}_{ij}^{(n)}\|}\right)\mathbf{r'}_{ij}^{(n)} + c_{ij}\mathbf{v'}_{ij}^{(n)}\right] + \mathbf{Fe}_i\left(t^{(n+1)}\right)}{m_i + \sum_{j\in S_i}\left(c_{ij}\delta\Delta t + k_{ij}\beta\Delta t^2\right)}, \tag{3}$$

$$\mathbf{v}_i^{(n+1)} = \mathbf{v}_i^{(n)} + (1-\delta)\mathbf{a}_i^{(n)}\Delta t + \delta\mathbf{a}_i^{(n+1)}\Delta t, \tag{4}$$

$$\mathbf{r}_i^{(n+1)} = \mathbf{r}_i^{(n)} + \mathbf{v}_i^{(n)}\Delta t + (0.5-\beta)\mathbf{a}_i^{(n)}\Delta t^2 + \beta\mathbf{a}_i^{(n+1)}\Delta t^2, \tag{5}$$

where δ and β are parameters for controlling acceleration changes between times $t^{(n)}$ and $t^{(n+1)}$. $\mathbf{r'}_{ij}^{(n)}$ and $\mathbf{v'}_{ij}^{(n)}$ can be expressed using acceleration $\mathbf{a}_{ij}^{(n)}$ of j relative to i

$$\mathbf{r'}_{ij}^{(n)} = \mathbf{r}_{ij}^{(n)} + \mathbf{v}_{ij}^{(n)}\Delta t + (0.5-\beta)\mathbf{a}_{ij}^{(n)}\Delta t^2, \tag{6}$$

$$\mathbf{v'}_{ij}^{(n)} = \mathbf{v}_{ij}^{(n)} + (1-\delta)\mathbf{a}_{ij}^{(n)}\Delta t. \tag{7}$$

Computation accuracy and stability depend on parameters δ and β [7]. In this paper, we choose $\delta = 1/2$ and $\beta = 1/4$ to enable unconditionally stable computation.

2.2 Cutting and Opening the Stomach

The stomach model is cut and stretched until its inner surface becomes observable. First, we manually input a cutting line on the model. Any parts of the stomach can be cut and removed, however, an usual cutting line is based on the rule defined in [6]. This rule requires two cuts that remove the cardia and pylorus of the stomach and a cut along its greater curvature. Cutting is implemented as the removal of mass points and Voigt elements in the hexahedra that coincide with the cutting line. Next, we apply the following stretching force to every mass point i near the cutting line

$$\mathbf{Fo}_i(t) = \alpha\big(\mathbf{Po}_i - \mathbf{r}_i(t)\big) \;/\; \|\mathbf{Po}_i - \mathbf{r}_i(t)\|, \tag{8}$$

where $\mathbf{r}_i(t)$ is the position of the mass point, $\mathbf{Po}_i$ is a control point specified in advance, and α is a constant representing the magnitude. Finally, deformation of the model is achieved by iteratively computing Eqs. 3, 4, and 5 using $\mathbf{Fo}_i(t)$ as $\mathbf{Fe}_i(t)$.

2.3 Flattening the Stomach Wall Using Surface Normals

Flattening forces driven by surface normals are introduced to direct the opened stomach onto a plane. First, we generate this so-called supporting plane using the coordinates and normals of the mass points allocated at vertices of hexahedron faces forming the stomach outer surface. Let us denote a set of these mass points as S_V. For each mass point i ($i \in S_\mathrm{V}$) a normal $\mathbf{K}_i$ is computed as a normalized sum of the normals of the faces that form the outer surface and share mass point i. The basepoint $\mathbf{B}_\Pi$ and the normal $\mathbf{N}_\Pi$ of the plane Π (defined by $(\mathbf{x} - \mathbf{B}_\Pi)\cdot\mathbf{N}_\Pi = 0$) are determined as follows :

$$\mathbf{N}_\Pi = \sum_{i\in S_\mathrm{V}} \mathbf{K}_i \;/\; \|\sum_{i\in S_\mathrm{V}} \mathbf{K}_i\| \quad , \quad \mathbf{B}_\Pi = \arg\max_{\mathbf{r}_i,\ i\in S_\mathrm{V}} (\mathbf{r}_i \cdot \mathbf{N}_\Pi)\,. \tag{9}$$

Next, we apply the following flattening force to every mass point i ($i \in S_\mathrm{V}$) to direct it onto the supporting plane :

$$\mathbf{Fu}_i(t) = \begin{cases} 0 & (\lambda_i \le 0) \\ \mu f_\mathrm{b}\mathbf{K}_i(t) & (0 < \lambda_i \le \lambda_\mathrm{b}), \\ \mu\|\mathbf{H}_i(t)\|\mathbf{K}_i(t) & (\text{otherwise}) \end{cases} \tag{10}$$

where $\lambda_i \equiv \mathbf{K}_i(t) \cdot \mathbf{N}_{\Pi}$. $\mathbf{H}_i(t)$ is a vector heading from $\mathbf{r}_i(t)$ in direction $\mathbf{K}_i(t)$ to its intersection point with Π. μ and f_{b} are two parameters for the magnitude control of $\mathbf{Fu}_i(t)$, while λ_{b} is a threshold for the magnitude of $\mathbf{Fu}_i(t)$. Deformation of the model is achieved by iteratively computing Eqs. 3, 4, and 5 using $\mathbf{Fu}_i(t)$ as $\mathbf{Fe}_i(t)$, until $\sum_{i \in S_{\mathrm{V}}} \|\mathbf{Fu}_i(t)\| \ / \ |S_{\mathrm{V}}| < \epsilon_{\mathrm{b}}$ is satisfied, where ϵ_{b} is a threshold and $|S_{\mathrm{V}}|$ is the size of S_{V}. To keep the model lying on the supporting plane, we calculate collision detection and response for any mass point that collides with the plane.

3 Results and Discussion

3.1 Comparison of Computation Stability with the Euler Method

We simulated deformation of a phantom model to compare the stability and computation time with the Euler method. Our phantom model consists of 1,386 mass points and 10,435 Voigt elements which were generated from a brick-like dataset containing $10 \times 20 \times 5$ voxels with $d = 1$, $m = 1$, $k = 9.87$, and $c = 0.13$. We applied streching forces of same magnitude to 4 mass points at 4 corners of the model until $t = 1.0$ then released. Five snapshots of the model simulated with $\Delta t = 0.02$ are shown in the upper row of Fig. 2. From $t = 16.0$, the model computed by the Euler method (darkly depicted) was collapsed, while the model computed by the Newmark-β method (brightly depicted) mostly preserved its shape. To gain the same stability by the Euler method, we had to choose $\Delta t = 0.0005$ (the lower row of Fig. 2). The computation time then became about 35 times that by the Newmark-β method with $\Delta t = 0.02$. These results shows that the Newmark-β method is very effective for simulating fast and accurate image deformation.

3.2 Unfolding the Stomach from Preoperative CT Images

We generated unfolded views from fifteen cases of CT image datasets and compared with those generated by the conventional method [2] from several aspects such as flatness of the unfolded stomach walls, reproduction rate of their luminal surface, virtual gastroscopic images, and resected specimens. Stomach walls were modeled with $d = 8$, $m = 1$, $k = 39.48$, and $c = 3.14$. Parameters and thresholds for computation are : $\alpha = 94.75$, $\Delta t = 0.1$, $\mu = 0.25$, $f_{\mathrm{b}} = 80.0$, $\lambda_{\mathrm{b}} = 0.5$, $\epsilon_{\mathrm{b}} = 5.0$. The *flatness* d_{Π} of the unfolded stomach wall and the *reproduction rate* R_s of its luminal surface are computed as

$$d_{\Pi} = \max_i \{(\mathbf{p}_i - \mathbf{B}_{\Pi}) \cdot \mathbf{N}_{\Pi}\} - \min_i \{(\mathbf{p}_i - \mathbf{B}_{\Pi}) \cdot \mathbf{N}_{\Pi}\}, \tag{11}$$

$$R_s = (1 - N_{\mathrm{CS}}/N_{\mathrm{S}}) \times 100, \tag{12}$$

where $\mathbf{p}_i$ is the position of voxel i in the stomach wall region, N_{S} is the number of voxels belonging to the luminal surface region, and N_{CS} denotes the number

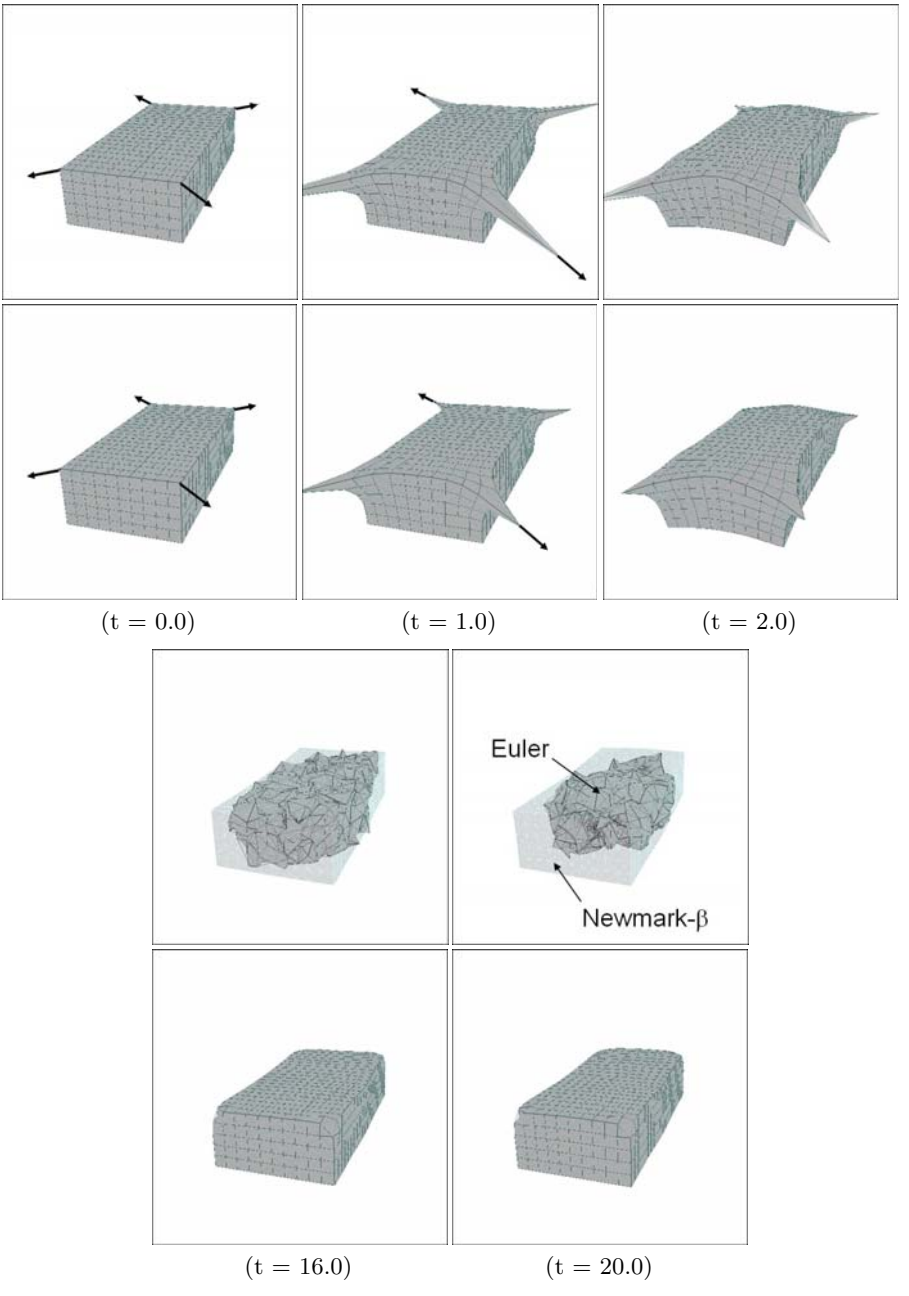

Fig. 2. Comparison of computation stability in simulating deformation of a phantom model using the same force magnitude and time step. Upper row : $\Delta t = 0.02$, lower row: $\Delta t = 0.0005$. Arrows illustrate stretching forces.

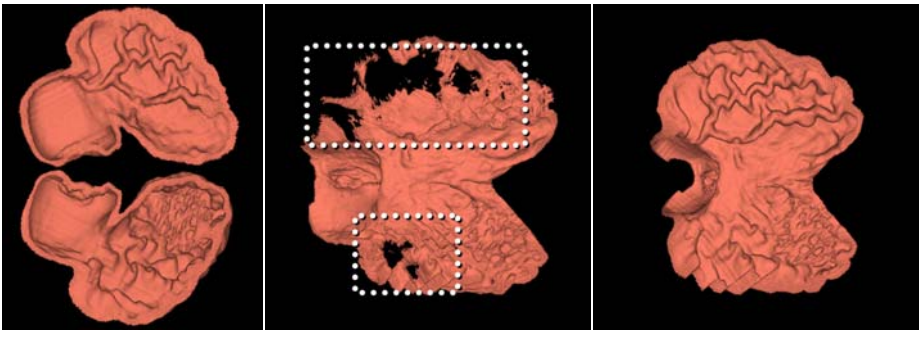

Fig. 3. Unfolding results under the same force magnitude ($\alpha = 15.0$) and time step ($\Delta t = 0.1$). (a): divided view, (b): unfolded view by Mori et al.'s method [2], (c): unfolded view by our method. Dashed rectangles indicate areas in which luminal surface was incorrectly reproduced due to collapse of hexahedra.

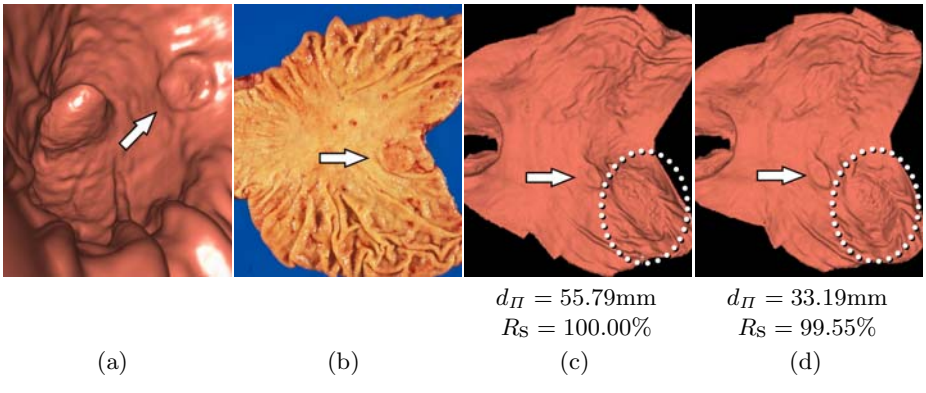

Fig. 4. Unfolding results with/without the proposed flattening process. (a): virtual gastroscopic view, (b): resected specimen, (c): unfolded view without flattening, (d): unfolded view with flattening. Dashed ellipses indicate concave areas in which unfolding is improved by the flattening process. Arrows indicate a cancer region.

of voxels that belongs to both the luminal surface region and the hexahedra collapsed during deformation.

An unfolded view generated by our method (without the flattening process) and that by the conventional method [2] using the same force magnitude ($\alpha = 15.0$) and time step ($\Delta t = 0.1$) are shown in Fig. 3. It can be seen from the unfolded view generated by the conventional method that two regions containing 49% of the luminal surface were not correctly reproduced (Fig. 3-(b)), while only

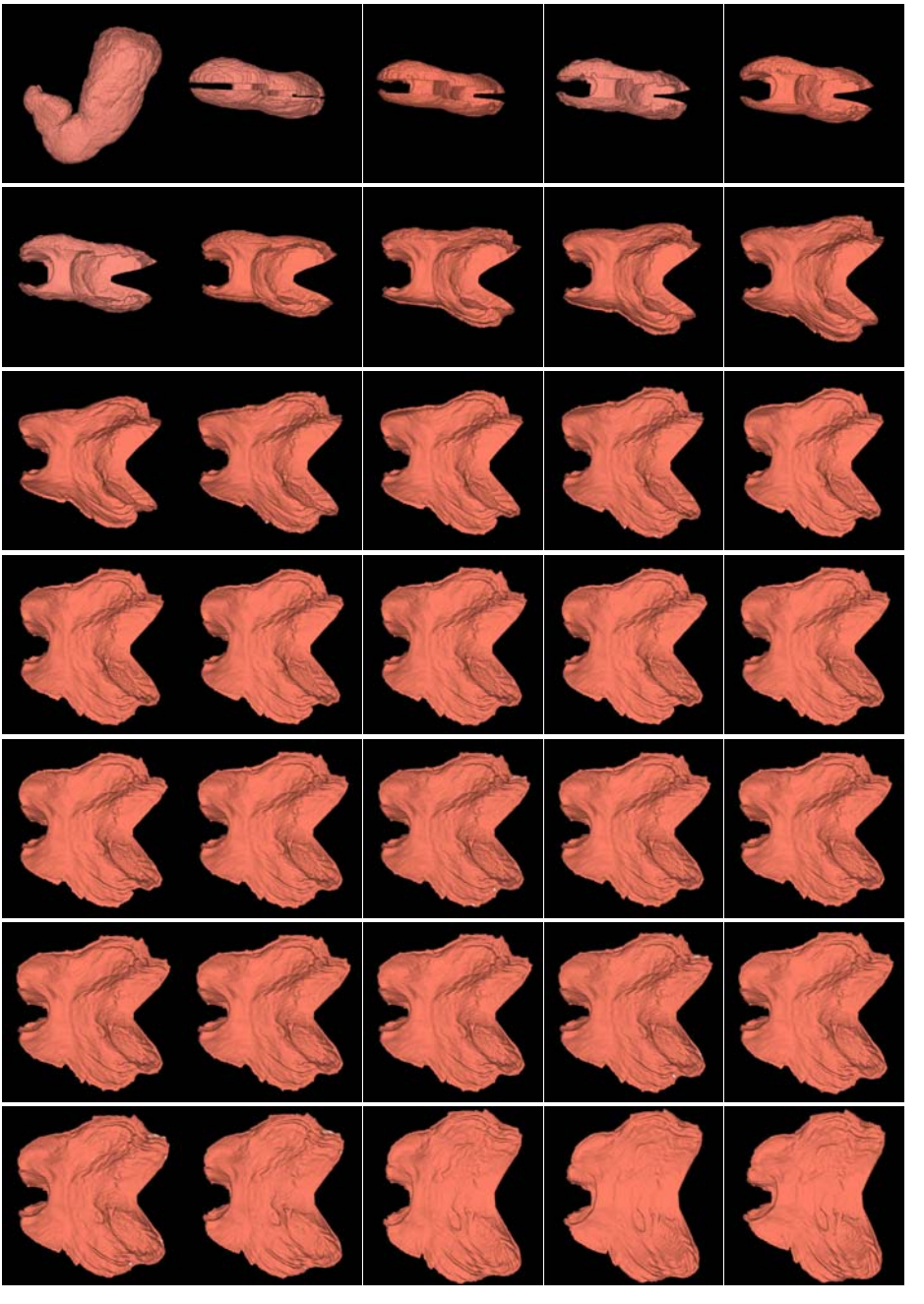

Fig. 5. Some views obtained in time sequence during simulation. (1): initial view, (2): cut view, (3)-(30): stretched views, (31)-(35): flattened views. All views except (1) were generated from the same viewpoint and view direction.

1% of the luminal surface was not reproduced by our method (Fig. 3-(c)). We also found that the conventional method gained 99% reproduction rate only with $\alpha \leq 0.15$. The computation time then became about 5 times that by our method.

Another example of unfolded views generated by our method with and without the flattening process is shown in Fig. 4. In the unfolded view generated without the flattening process, there are some concave areas in which the stomach was not unfolded to a flat shape (Fig. 4-(c)). By introducing the flattening process, the flatness of the stomach wall decreased from 55.79 mm to 33.19 mm, and about 1% of the luminal surface was not correctly reproduced. Some snapshots taken during the unfolding process are shown in Fig. 5.

By using Voigt elements for the elastic modeling of the stomach and the Newmark-β method for image deformation, our method can reconstruct image data more accurately. The unreproduced luminal surface region is 1%, which is small enough not to be detected on the unfolded views by human eyes. We presented the unfolded views from twelve datasets for surgical planning. They were considered to have well reproduced lesions as well as fold patterns observed in virtual gastroscopic images and disected specimens (Fig. 4). This is very meaningful for image-guided diagnosis in which the status of the lumen provides various information. By introducing flattening forces determined from surface normals, we can take into account the relationship between the stomach and the supporting plane for shape deformation. Thus, concave parts of the stomach, which are difficult to unfold by the conventional method, can be flattened, generating views of more precise information of the luminal surface.

4 Conclusion and Future Work

We have presented an improved method for generating unfolded stomach views based on flattening forces and stable volumetric image deformation. Experimental results showed that our method can generate unfolded views in which stomach walls are flattened better and their luminal surface is reproduced more accurately. We believe that our method can be used as one basic visualization technique for intuitive observation of the stomach from preoperative CT images. Our future work includes further evaluation of unfolded views and application to a larger number of datasets. Especially, evaluation of geometric distortions of the luminal surface, investigation of the relationship between the quality of unfolded views and the resolution of CT images, as well as quantitative comparison between unfolded views and resected stomach specimens are good issues to challenge.

Acknowledgments

We would like to thank Dr. Shigeru Nawano of the National Cancer Center East, Japan and Dr. Kunihisa Miyagawa of the National Cancer Center for providing CT images and useful comments from a medical viewpoint. We also thank

Dr. Michitaka Fujihara of the Faculty of Medicine, Nagoya University and Dr. Kazunari Misawa of Graduate School of Medicine, Nagoya University for evaluating a number of unfolded views presented in this paper and their supervision. Special thanks to the reviewers of this paper for their useful comments and suggestions. Parts of this research were supported by the Grant-In-Aid for Scientific Research from the Ministry of Education, the 21st century COE program, the Grant-In-Aid for Scientific Research from Ministry of Education, Culture, Sports, Science and Technology, Japan Society for Promotion of Science of Japanese Government, and the Grand-In-Aid for Cancer Research from the Ministry of Health and Welfare of Japanese Government. We are also supported by the Kayamori Foundation of Informational Science Advancement.

References

1. J. H. Kim, S. H. Park, H. S. Hong, and Y. H. Auh, "CT gastrography," Abdominal Imaging, Vol. 30, No. 5, pp. 549–517, 2005.
2. K. Mori, H. Oka, T. Kitasaka, Y. Suenaga, and J. Toriwaki, "Virtual Unfolding of the Stomach Based on Volumetric Image Deformation," MICCAI 2004, LNCS 3217, pp. 389–396, 2004.
3. G. Wang, E. G. McFarland, B. P. Brown, and M. W. Vannier, "GI Tract Unraveling with Curved Cross Section," IEEE Trans. Med. Imaging, Vol. 17, No. 2, pp. 318–322, 1998.
4. L. Zhu, S. Haker, and A. Tannenbaum, "Flattening Maps for the Visualization of Multibranched Vessels," IEEE Trans. Med. Imaging, Vol. 24, No. 2, pp. 191–198, 2005.
5. S. Cotin, H. Delingette, and N. Ayache, "Real-time elastic deformations of soft tissues for surgery simulation," IEEE Trans. Vis. Comput. Graphics, Vol. 5, No. 1, pp. 62-73, 1999.
6. Japanese Gastric Cancer Association ed., "Japanese Classification of Gastric Carcinom, 13th ed.," Kanehara Publishing Inc., Tokyo, Japan, 1999.
7. N. M. Newmark, "A Method of Computation for Structural Dynamics," Proc. ASCE, Vol. 85, No. EM3, pp. 67-94, 1959.